Physica Scripta. Vol. T115, 1032–1034, 2005

# A Study of Transition Metal K Absorption Pre-Edges by Resonant Inelastic X-Ray Scattering (RIXS)

P. Glatzel*[1,2], U. Bergmann[3], F. M. F. de Groot[1], Bert M. Weckhuysen[1] and S. P. Cramer[2,3]

[1]Department of Inorganic Chemistry and Catalysis, Utrecht University, 3584 CA Utrecht, The Netherlands
[2]Department of Applied Science, University of California, Davis, California 95616, USA
[3]Physical Biosciences Division, Lawrence Berkeley National Laboratory, Berkeley, California 94720, USA

*Received June 26, 2003; accepted January 30, 2004*

PACS numbers: 78.70.Ck, 78.70.Dm, 78.70.En, 71.70.−d, 71.70.Ch, 71.15.−m

## Abstract

The K absorption pre-edge structure arises from excitations into the lowest unoccupied states that are partly formed by metal 3d orbitals. The pre-edge energy position, intensity and spectral shape can give valuable insight into the metal site symmetry and electronic configuration. The excited electronic states that form the absorption pre-edge subsequently decay radiatively. This fluorescence decay can be recorded using a crystal spectrometer that has a similar energy bandwidth as the incident beam. Plotting the fluorescence intensity versus incoming and outgoing energy yields three-dimensional plots that offer numerous possibilities for further analysis. In this paper we show that resonant inelastic X-ray scattering (RIXS) considerably facilitates separation of the K pre-edge structure from the strong dipole allowed transitions at higher incident energies. Previously unobserved spectral features could be revealed. The spectra along the energy transfer axis contain information on the electronic structure that is complementary to K-edge absorption spectroscopy.

## 1. Introduction

The electronic states that form an absorption spectrum are resonantly excited states that subsequently decay. The released energy can be carried either by an electron that is excited into the continuum (resonant Auger effect) or by a photon (resonant X-ray scattering or RXS). A review of the resonant Auger effect was published by Armen [1]. A large body of work already exists on resonant X-ray scattering that was reviewed comprehensively by Gel'mukhanov and Ågren as well as Kotani and Shin [2]. We will focus in this article on resonant inelastic X-ray scattering (RIXS) at the transition metal K absorption pre-edges where only few studies have been done up until now.

## 2. The RIXS plane

After resonant excitation of a 1s electron, the subsequent radiative decay with the highest probability is a 2p to 1s (K$\alpha$) transition. The 3p to 1s (K$\beta$) transitions are about a factor 8 weaker [3]. An expression for the RIXS spectrum $F(\Omega, \omega)$, where $\Omega$ and $\omega$ are, respectively, the incident and emitted photon energy, can be derived from the differential cross section that describes the inelastic X-ray scattering process [2]. It is giving by

$$F(\Omega,\omega) = \sum_f \left| \sum_i \frac{\langle f|T_2|i\rangle\langle i|T_1|g\rangle}{E_g - E_i + \Omega - i\frac{\Gamma_K}{2}} \right|^2 * \frac{\Gamma_L/2\pi}{(E_g - E_f + \Omega - \omega)^2 + \frac{\Gamma_L^2}{4}}. \quad (1)$$

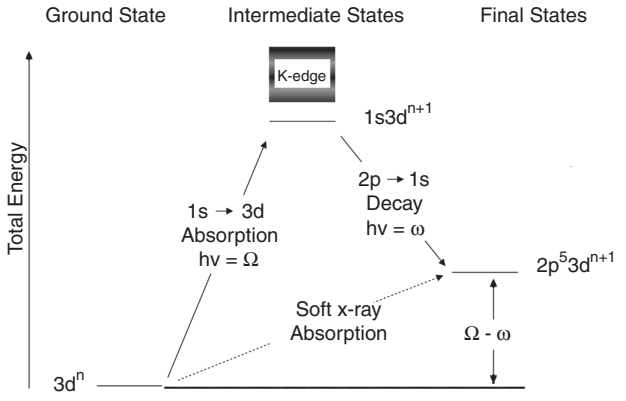


*Fig. 1.* Energy scheme for 1s2p RIXS in a transition metal ion. The vertical axis indicates the total energy of the electron configuration. For simplicity, atomic configurations are used and only 1s to 3d excitations are shown.

The intermediate state $|i\rangle$ is reached from the ground state $|g\rangle$ via a transition operator $T_1$. In a simplified picture using atomic configurations we can write $|g\rangle = 3d^n$ and $|i\rangle = 1s3d^{n+1}$, *i.e.* a 1s electron is resonantly excited into a 3d orbital (Figure 1). The intermediate states $|i\rangle$ in RIXS spectroscopy are the final states in conventional absorption spectroscopy. The spherical ($SO_3$) symmetry of the atomic 3d orbitals branches to the lower symmetry at the metal site. $T_1$ identifies with the quadrupole transition operator if the scattering atom is in centrosymmetric coordination (*e.g.* $O_h$ symmetry). If the symmetry is reduced, *e.g.* to square pyramidal ($C_{4v}$) or tetrahedral ($T_d$), $T_1$ obtains some dipole contribution. In this case, the crystal field split 3d orbitals partly belong to the same irreducible representation of the point group as the metal 4p orbitals. The states can therefore mix and transitions from 1s to the 3d4p mixed states are dipole allowed [4]. The ratio of the dipole to the quadrupole contribution can be determined in single crystalline samples by analyzing the angular dependence of the absorption coefficient using linear polarized light [5] or by studying anomalous diffraction [6].

The final states are reached via a 2p or 3p to 1s dipole transition. The electron configurations of the RIXS final states are identical to the soft X-ray L-edge ($2p^53d^{n+1}$) and M-edge ($3p^53d^{n+1}$) absorption final states. However, the RIXS process is described by two transition matrix elements (cf. Equation (1)) that are connected coherently while an absorption spectrum arises from one transition (cf. Figure 1). Thus, the intensities in the fine structure of the spectra resulting from spin-orbit and electron-electron interactions as well as crystal field splittings might differ between K pre-edge RIXS and soft X-ray absorption.

*current address: European Synchrotron Radiation Facility, 38000 Grenoble, France; e-mail: glatzel@esrf.fr

The incident energy $\Omega$ as well as the emitted energy $\omega$ are varied in a RIXS experiment. The recorded intensity is proportional to $F(\Omega, \omega)$ and is thus plotted versus a two-dimensional grid. The overall spectra are best displayed in contour plots. In order to assign the total energy of an electronic state to the axes of the contour plots we will use the energy transfer or final state energy $\Omega - \omega$ as opposed to the emitted energy $\omega$ (Figure 1). The energy transfer axis relates to the excitation energy in L- and M-edge absorption spectroscopy, respectively. The lifetime broadenings $\Gamma_K$ for the intermediate states and $\Gamma_f (f = \mathrm{L}, \mathrm{M})$ for the final states then apply in the $\Omega$ and $\Omega - \omega$ direction, respectively. Scans with constant emission energy (CEE) represent diagonal cuts through the $(\Omega, \Omega - \omega)$ RIXS plane. They are usually plotted versus the incident energy axis and then exhibit a line sharpening effect when compared to an absorption scan [7, 8].

The instrumental broadenings stretch in the diagonal (incident beam) and vertical (emitted beam) direction in the $(\Omega, \Omega - \omega)$ plane. Resonant 1s excitations into localized orbitals with a discrete energy occur along a diagonal line if we neglect many-electron transitions. Spectral features off of this diagonal line towards larger energy transfer are due to electron-electron interactions in the final state between the unpaired p-electron and the valence shell. Continuum excitations or excitations into delocalized final states with a broad energy band can be viewed as an infinite number of resonant excitations infinitely close to each other. In the $(\Omega, \Omega - \omega)$ plane they thus appear as a diagonal streak [9].

## 3. Experiment

The spectra were recorded at the BioCAT beamlime 18 ID at the Advanced Photon source. The total incident flux in the first harmonic of the undulator radiation was on the order of $10^{12}$ to $10^{13}$ photons/s depending on the incident energy monochromator crystal. For incident energies below 8 keV a cryogenically cooled Si(111) double crystal monochromator was employed. Above 8 keV (Ni K-edge) the Si(400) Bragg reflection was used. The fluorescence spectrometer features up to 8 analyzer crystal [10]. The following Bragg reflections were used: Ge(331) for V K$\alpha$, Ge(333) for Mn K$\alpha$, Ge(620) for Fe K$\beta$ and Si(620) for Ni K$\alpha$. The total data acquisition time to record one RIXS plane was 2–4 hours. Careful radiation damage studies were performed for each sample. Radiation sensitive samples were measured in a He-flow cryostat in an exchange gas surrounding. The RIXS plane was constructed by recording CEE scans (2–30 seconds each in 'on-the-fly' mode) for different emission energies. The beam position on the sample was changed with every scan and the spectra were corrected for variations in sample concentrations.

## 4. Results

A series of Ni coordination complexes shows the pre-edge shift with Ni oxidation state (Figure 2). While the K pre-edge yields identical spectra for Ni(II) high-spin and low-spin we can clearly identify the different Ni species in the energy transfer direction. The 1s2p RIXS plane for $NiF_2$ ($3d^8$ in $O_h$ symmetry) shows one K pre-edge resonance and a pronounced asymmetry towards the energy transfer direction due to (2p,3d) multiplet interactions. The high energy shoulder in the energy transfer direction has been used as a diagnostic of high-spin Ni(II) [11]. The K pre-edge is nearly invisible in the conventional absorption scan of the Ni(III) complex. Using the RIXS technique we can clearly resolve two strong resonances [12].

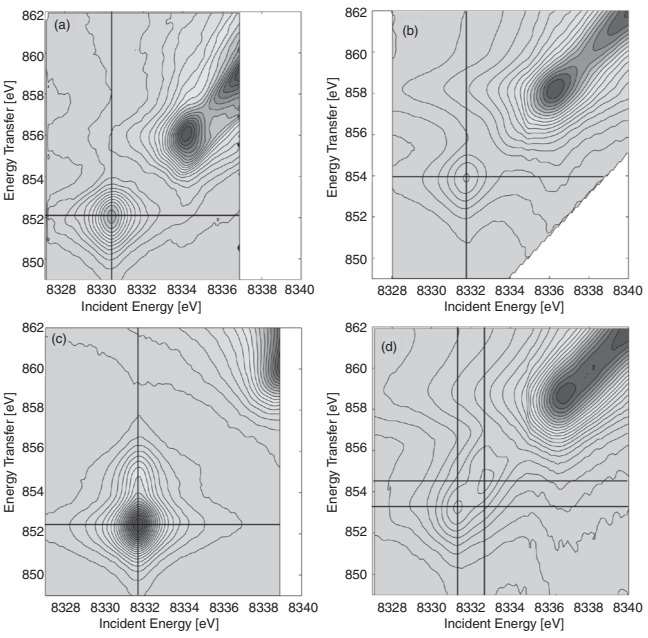


*Fig. 2.* $2p_{3/2}$ final states in the 1s2p RIXS contour plots for Ni coordination complexes: (a) Ni(I) in $[PhTt^{tBu}]NiCO$, Ni(II) (b) low-spin (ls) in $(Ph_4As)_2Ni(S_2C_2(CF_3)_2)_2$, Ni(II) (c) high-spin (hs) in $NiF_2$ and (d) Ni(III) low-spin in $[Ni(\eta^4\text{-DEMAMPA-DCB})]^-$. The vertical (constant incident energy) and horizontal (constant final state energy) lines indicate the lowest 1s to 3d resonances.

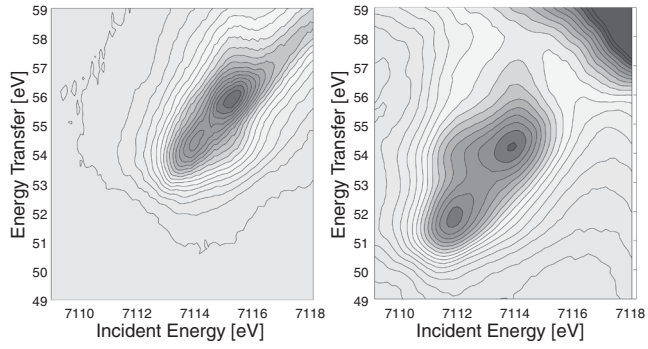


*Fig. 3.* 1s3p RIXS planes of $Fe_2O_3$ (left) and $Fe_{0.05}Mg_{0.95}O$ (right).

The 1s3p RIXS planes in Fe(II) ($Fe_{0.05}Mg_{0.95}O$) and Fe(III) ($\alpha$-$Fe_2O_3$) in octahedral geometry show the pre-edge shift with oxidation state that we already observed for Ni. This is well documented in the literature (Figure 3) [13]. The crystal field splitting separates the two peaks for Fe(III) in $Fe_2O_3$ with $^5T_{2g}$ and $^5E_g$ symmetry. A theoretical analysis of the multiplet structure yields three 1s to 3d resonances for Fe(II) in $Fe_{0.05}Mg_{0.95}O$ with $^4T_1$, $^4T_2$ and $^4T_1$ terms [14]. A pronounced asymmetry relative to the diagonal towards larger energy transfer can be observed for the $Fe_{0.05}Mg_{0.950}O$ complex. This indicates strong (3p,3d) final state interactions. The RIXS spectra indicate that the center resonance with $^4T_2$ symmetry exhibits the strong final state interactions.

For a detailed analysis of the pre-edge features it is necessary to subtract the background due to the K main edge. We developed a procedure that fits horizontal cuts through the RIXS plane at constant energy transfer to Voigt line profiles [15]. The fit yields a background plane that can be subtracted from the experimental RIXS plane. An example is shown for MnO in Figure 4 where we also show ligand field multiplet calculations that reproduce

 

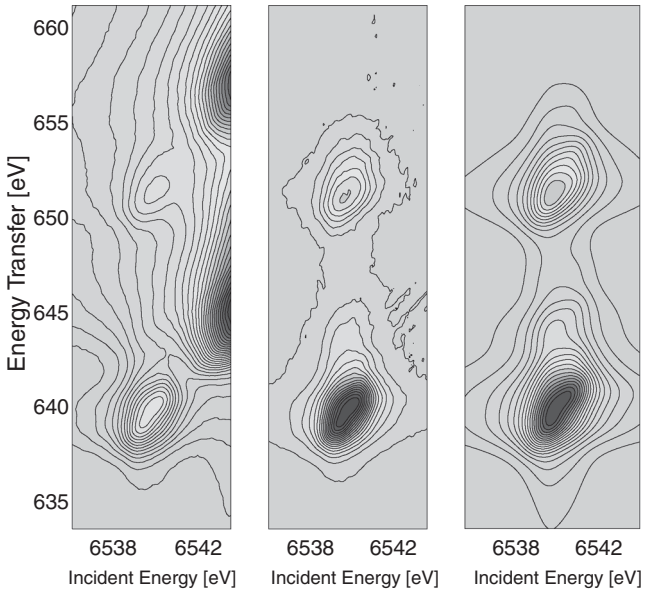


*Fig. 4.* 1s2p RIXS plane of MnO before (left) and after (center) subtraction of the K main edge together with ligand field multiplet calculations (10 Dq = 1.1 eV). The applied lifetime broadenings are $\Gamma_K = 1.1$ eV and $\Gamma_L = 0.5$ eV for the intermediate and final state, respectively, as well as 1.0 eV and 0.8 eV for the instrumental lifetime broadenings of the incident and the emitted X-rays. The features at 640 eV and 652 eV are the $2p_{3/2}$ and $2p_{1/2}$ final states, respectively.

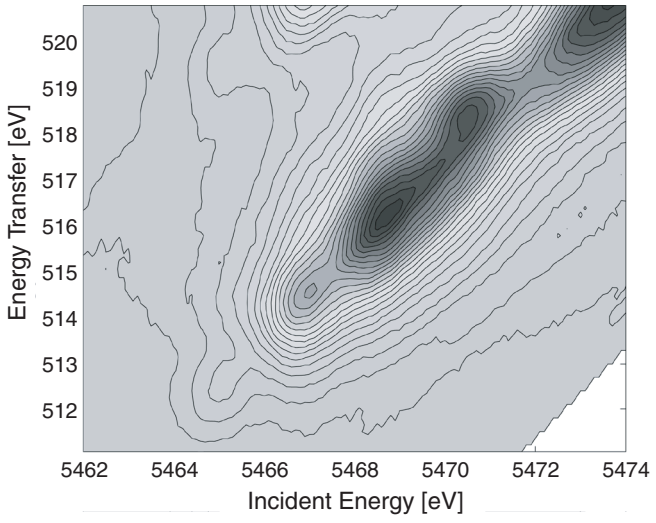


*Fig. 5.* $2p_{3/2}$ final states in the 1s2p RIXS plane of $VF_4$.

the experimental spectral shape after edge subtraction. The MnO $1s2p_{3/2}$ RIXS spectra can be fitted to two 1s resonances that are separated by the crystal field splitting similar to $Fe_2O_3$. This is consistent with 1s to 3d ligand field multiplet calculations for high-spin Mn(II) in $O_h$ symmetry and thus indicates that quadrupole transitions contribute to the pre-edge intensity. The $2p_{3/2}$ final states exhibit a shoulder on the high energy transfer side that also appears in soft X-ray L-edge spectroscopy for high-spin Mn(II) compounds [16].

The K pre-edge of $VF_4$ presents a nice example for the interplay between crystal field and multiplet splittings. Both have approximately the same magnitude and result in four almost equally separated pre-edge structures (Figure 5) [17]. The two strong resonances at high incident energies appear to be further split. This could be indicative of the Jahn-Teller splitting in the $t_{2g}$ orbitals.

## 5. Summary

RIXS spectroscopy enables to separate the K pre-edge from the main edge with a considerably higher accuracy than in conventional absorption spectroscopy. Previously unobserved spectral feature could be resolved. The energy transfer spectra contain information on the electronic structure that is complementary to the K pre-edge. Ligand field multiplet calculations can simulate the spectral features.

## Acknowledgement

This work was supported by the National Institutes of Health Grants GM-44380 and the DOE Office of Biological and Environmental Research. Use of the Advanced Photon Source was supported by the U.S. Department of Energy, Basic Energy Sciences, Office of Science, under contract No. W-31-109-ENG-38. BioCAT is a National Institutes of Health-supported Research Center RR-08630.

## References

1. Armen, G. B., Aksela, H., Åberg, T. and Aksela, S., J. Phys. B-At. Mol. Opt. Phys. **33**, R49 (2000).
2. Gel'mukhanov, F. and Ågren, H., Phys. Rep.-Rev. Sec. Phys. Lett. **312**, 91 (1999); Kotani, A. and Shin, S., Rev. Mod. Phys. **73**, 203 (2001).
3. Kortright, J. B. and Thompson, A. C., "X-ray Data Booklet". (Edited by Thompson, A. C. and Vaughan, D.) (Lawrence Berkeley National Laboratory, Berkeley 2001).
4. Griffith, J. S., "The theory of transition-metal ions". (University Press, Cambridge Eng. 1964).
5. Bocharov, S., Kirchner, T., Drager, G., Sipr, O. and Simunek, A., Phys. Rev. B **6304** art. no.-045104 (2001), Uozumi, T. *et al.*, Europhys. Lett. **18**, 85 (1992).
6. Finkelstein, K. D., Shen, Q. and Shastri, S., Phys. Rev. Lett. **69**, 1612 (1992).
7. de Groot, F. M. F., Krisch, M. H. and Vogel, J., Phys. Rev. B **66** art. no.-195112 (2002).
8. Carra, P., Fabrizio, M. and Thole, B. T., Phys. Rev. Lett. **74**, 3700 (1995).
9. Glatzel, P. and Bergmann, U., Coord. Chem. Rev., in press (available on the web).
10. Bergmann, U. and Cramer, S. P., SPIE Proc. **3448**, 198 (1998).
11. Wang, H. X. *et al.*, J. Am. Chem. Soc. **122**, 10544 (2000).
12. Glatzel, P. *et al.*, J. Am. Chem. Soc. **124**, 9668 (2002).
13. Wilke, M., Farges, F., Petit, P. E., Brown, G. E. and Martin, F., Am. Miner. **86**, 714 (2001).
14. Westre, T. E. *et al.*, J. Am. Chem. Soc. **119**, 6297 (1997).
15. Glatzel, P. *et al.*, J. Am. Chem. Soc. **126**, 9946 (2004).
16. Cramer, S. P. *et al.*, **113**, 7937 (1991).
17. Solomonik, V. G. and Pogrebnaya, T. P., Russ. J. Inorg. Chem. **46**, 1851 (2001).